

## Scour Protection Around Bridge Pier Using Based Ramp

Tussanun Thunyaphun<sup>1,\*</sup> Duangrudee Kositgittiwong<sup>2</sup> and Chaiwat Ekkawatpanit<sup>3</sup> Rachapol Sukjan<sup>4</sup>

<sup>1,2,3,4</sup> Department of Civil Engineering, Faculty of Engineering, King Mongkut's University of Technology Thonburi, Bangkok, THAILAND

\*Corresponding author; E-mail address: Tussanun.nud@gmail.com

### Abstract

The purposes of this study will innovate the scour protection system around bridge piers reducing the depth and size of scour by using based ramp protection. Bridge piers are substructure which strongly used to support bridges. It appears that one of the main causes of bridge pier failure is scour. Scour is a hydrodynamic process that remove the sediment around bridge piers caused by flow separation as well as vortexes developing also known as scour hole. For the reason, bridge piers able to fail in case there is not enough protection and attentive consideration. The experiments were carried out in the large-sized open-channel flume at KMUTT. The scour mechanism and the time-varied development of scour depth were studied. The based ramps for scour protection were designed and differentiated into four different size and shape in order to find the most effective protection and reduction for scour. Maximum depth and 12-measuring points around the curb of the scour hole were measured and collected. In the first 60 minutes, the measuring point reading was recorded every 10 minutes, and then every 30 minutes until reaching 120 minutes. The test results show the maximum scouring depth is increasing in the function of time. An unprotection pier without based ramp was conducted to be the reference. The cases with based ramp protection then carried out to compare and analyze the protection efficiency.

Keywords: Scour, Scour protection, Bridge pier, Based ramp

### 1. Introduction

Bridge piers are substructure which strongly used to support bridges. The collapse of which could be so tragic, leading to lose of many lives and potential millions in property damage. It appears that one of the main responsible for bridge pier damage is hydrodynamic scour. There is a study reports that more than

20% of pier failure and 70% of abutment damage in the total amount of 383 cases of bridge failure were caused by scour damage in the US 1973 [1].

Scour is a hydrodynamic process that remove the sediment around bridge piers caused by flow separation as well as vortexes developing also known as scour hole. For the reason, bridge piers able to fail in case there is not enough protection and attentive consideration. For the scour classification, there are three main types of scour categorized by the characteristic of it as general scour, contraction scour as well as local scour. Melville and Coleman reported that among these three types of scour, the local scour is mostly known as the most severe type of scour for bridge damage [2]. It caused by fast-moving water removing sediment due to the blockage of the bridge pier from around the bridge foundation, leaving behind scour holes where the bed material is carried away.

Creating scour countermeasures to protect and reduce bridge pier foundations from the scour and vortex problem has turned into an influential issue for the design and conservation of bridge piers located in erodible bed materials. Since the development of scour is influenced by a large number of variables for instant, the characteristic of flow, the shape and size of pier, the sediment characteristic, the function of time and the type of scour which can be classified into two main categories as the clear-water scour and the live-bed scour. The big different between these two types of scour is that the clear-water scour approaching flow does not carry any sediment whereas the live-bed scour do.

In this study, the physical experiments have been conducted in order to create a flow-altering countermeasure device named based ramp protection aiming for reduce scour depth and the width of the scour around bridge pier. Since their efficiencies in reducing scour are somehow related to the shape, dimension and geometric arrangement, the configurations of

based ramp protection device are compared and studied to seek for the sustainable long-term solutions to scour problems.

## 2. Short Overview in Scour Phenomenon

### 2.1 Scour mechanism

Since a pier foundation is built in the river or sea, the behavior of water flow around that area is changed turbulently leading to the different forms of fluid flow. There are a several main fluid flow that affect the occurrence of scour hole around bridge pier including downflow, horseshoe vortex and wake vortices as shown in Fig. 1 [3]. Each flow has different position and direction resulting in different behavior of scour hole. In detail, Downflow occurs when the water flow collides with the upper part of the pier pillar and it tend to move downward to the bottom part of the pier moving away bed material around the pier. For Horseshoe vortex, it occurs when the abstraction and flow acceleration at the front of the pile as shown in the profile view of Fig. 1, which is the result of the vertical gradient in stagnation pressure at the edge of the pile by increasing the depth of scour, the strength of this vortex is reduced. At downstream, behind the pier, the separation of flow happens and Wake vortices are formed. The moving characteristic of the Wake vortices is similar to storm swirling at the back of the pier. Lifting up bed material around the back of the flow causing the scour hole at the back of the pier as shown in the plan view of Fig. 1. The strength of wake vortex decreases rapidly by increasing the distance.

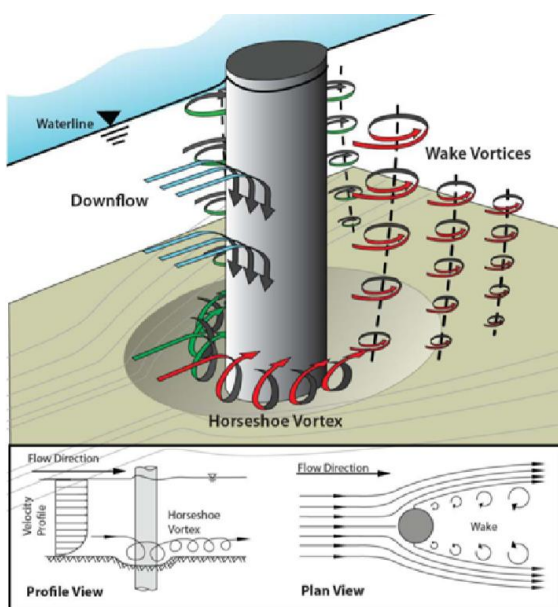


Fig. 1 Schematic Drawing of the Hydraulic Processes Causing Local Scour at a Cylindrical Pier [3]

In short, the concept of its occurrence is the rate of bed material removing is more than the rate of bed material transporting, clear-water scour exists. The maximum scour will be limited by the mechanism of sediment transportation. Any structure founded or built on the seafloor or riverbed can experiences common scour problems at downstream side such as surge barriers, bridges and abutments as shown in Fig. 2 [4].

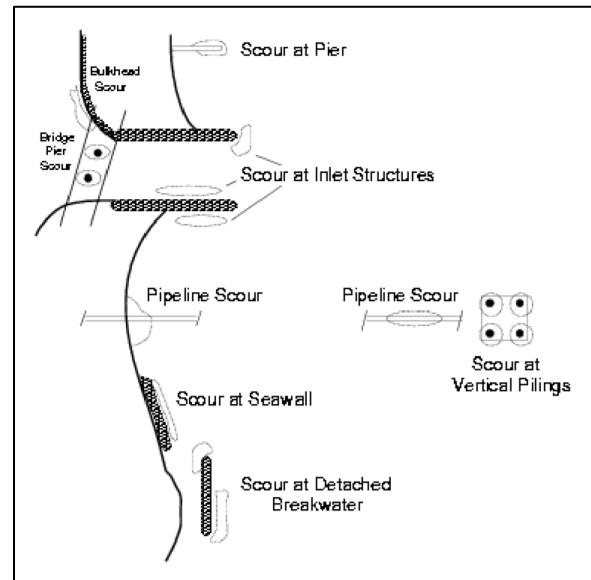


Fig. 2 Schematic Drawing of the Hydraulic Processes Causing Local Scour at a Cylindrical Pier [4]

### 2.2 Type of scour

Two scour types were classified based on the characteristic of scour movement especially for the general and local scour. The two types of the scour are the clear-water scour and the live-bed scour [1].

#### 2.2.1 Clear-water scour

Clear-water scour occurs when there is no movement of the bed material in the main channel of the upstream or when the floodplain is transported through the bridges such as coarse bed material streams, flat gradient streams in low flow and vegetated channels. Clear water scour conditions occur for both uniform and nonuniform sediments.

#### 2.2.2 Live-bed scour

Live-bed scour occurs oppositely to the clear-water scour. It occurs only for uniform sediments when the bed material is moving. It moves as contact sediment discharge and/or into the local scour holes.

Based on Fig. 3 [1], live-bed scour typically reaches its maximum faster than clear-water scour. This might be because of the occurrence of clear-water scour. It occurs mainly on coarse bed material or low flow channels. In fact, clear-water scour may not reach its maximum until after several floods. Also, maximum clear-water scour is about 10 percent greater than the equilibrium live-bed scour. Moreover, there is a reason from the theory of sediment transport of bed material that live bed scour fluctuate streams with a dune.

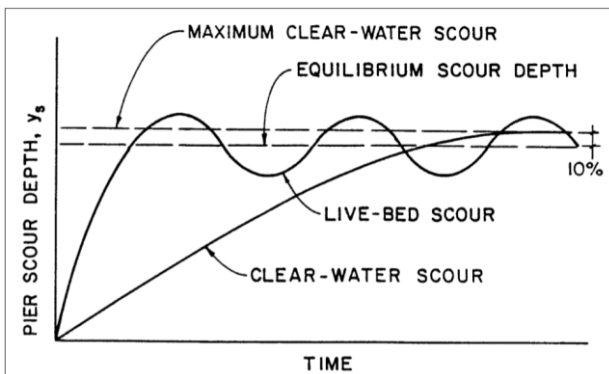


Fig. 3 Piers scour depth in a function of time [1]

### 2.3 Effects of specific parameters on scour

There are so many parameters affect the process and characteristic of the scour around bridge piers and also the flow pattern and flow velocity. As shown in Table 1 [6], the overview of scouring parameter that affect the behavior of the scour occurring around bridge pier has been illustrated in the table. Four different parts were classified including flow, fluid, bed material and geometry of pier shape. The fluid properties seem to be less influenced when literally compared to the flow characteristics. Moreover, there is just a small effect of bed material size and range on the scour depth development [7].

#### 2.3.1 Characteristic of flow pattern

Both of the flow pattern and the scour pattern near bridge pier is totally complicated. However, there are a couple authors has been explained about the behavior of the scour related the flow pattern for example Breusers and Raudkivi [7]. Also, Yeleğen and Uyumaz [8] have found from their research that It is easily seen from the study that equations which consider the flow velocity ratio provide improved and more accurate calculations than others. the ratio of flow velocity to the critical flow velocity is an important parameter in calculation of scour depth.

Table 1 The scouring parameters [6].

Categories	Parameter names
Fluid	Acceleration of gravity (m/s <sup>2</sup> )
	Fluid density (kg/m <sup>3</sup> )
	Kinematic viscosity (m <sup>2</sup> /s)
Flow	Flow depth (m)
	Mean flow velocity (m/s)
	Chézy coefficient (m <sup>1/2</sup> /s)
Bed material	Representative diameter of the bed material: d <sub>50</sub>
	Surface packing
	Multiple layers of different bed materials
Geometry	Cohesion of material
	Shape in a horizontal and vertical section
	Piers composed of different element
	A group of separate piers, without a footing

#### 2.3.2 Characteristic of bed parameters

From a geotechnical aspect, the stability of the upstream scour slope is of prime importance both during the scour process and in the final situation when equilibrium geometry has been attained. Sediment transport in the scour hole, soil particles in the filter structure below the bed protection can also be transported in both vertical and horizontal directions. The shape, the slopes of a scour hole and the maximum scour depth determine the volume of a scour hole and the minimum extent of a bed protection to prevent a local scour. The slope pattern of the scour has been studied by several researchers. Dargahi depicted that the slope of the scour hole developed around the bridge pier can be divided into three regions: upper, lower and the deepest part of the scour hole (close to the pier area) as shown in Fig. 4 [9].

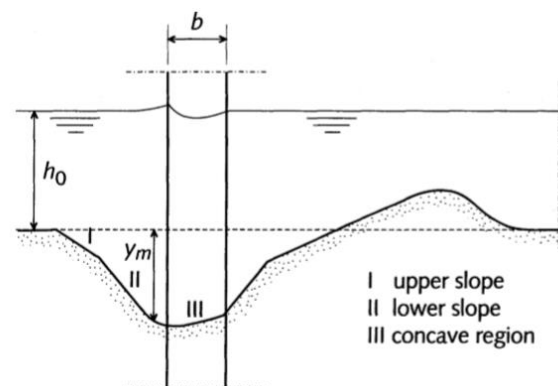


Fig. 4 The classification of position of scour [9]

### 2.3.4 Time scale

It is obvious that the process of scouring around bridge pier depends upon the function of time. Sometimes it has the big different scour shape when compare in the different period. Carstens divided the process of scouring as shown in Fig. 5 [10] into 4 phases including initial phase, development phase, stabilization phase and equilibrium phase. Normally, some process happened rapidly and the occurrence of the maximum scour depth is not always relevant to the time dependent description. Nevertheless, the time scale played an important role for some cases such as during the construction.

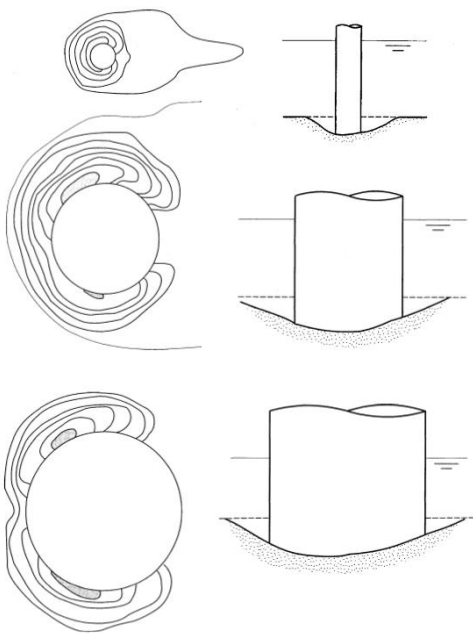


Fig. 5 Scour pattern in different phase [10]

## 2.4 Scour failure

Since there are a couple of relation between the scour pattern and parameters, the scour failure also has a lot of pattern depending on how the scour occurrence are caused and affect to the pier. Three main type of scour failure are mentioned as follows:

### 2.4.1 Sliding of main armor due to seabed scour

This type of scour failure occurs when the formation of the scour hole is close to the foot of the structure due to wave and current action. The toe is functioning as support for the main armor as long as the toe erosion does not cause undermining of the armor as shown in the Fig. 6. It also reduces the stabilizing forces causes slip failure to occur which results in sliding of armor.

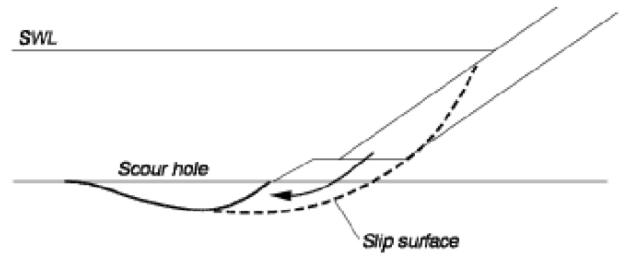


Fig. 6 Sliding of main armor due to seabed scour [4]

### 2.4.2 Scour in seabed, seaward tilt and settlement

Scour in front of a caisson due to waves and currents might cause seaward tilt and settlement of the caisson. The critical wave load situations are when deep wave troughs occur at the front of the caisson as shown in Fig. 7.

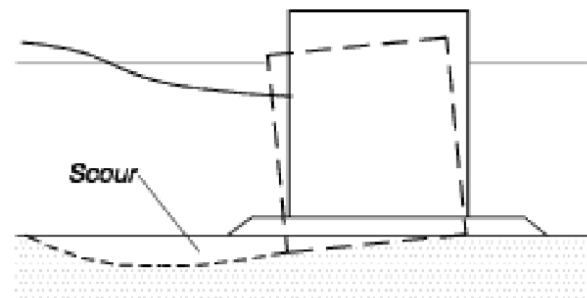


Fig. 7 Scour from seaward tilt and settlement [4]

### 2.4.3 Overturning and settlement of gravity walls

This type of scour will occur when the passive resistance and the bearing capacity of the foundation soil were reduced affecting the scour in front of the wall. The resulting load from the active backfill pressure, the high groundwater table and the weight of the wall cause a bearing capacity failure in the soil resulting in a forward overturning and some settlement of the wall as shown in Fig 8.



Fig. 8 Seaward overturning and settlement of gravity wall [4]

## 2.5 Scour protection

The careful consideration of the design of bridge piers for scour protection is totally important. The extent, elevation and detail of the scour protection should be carefully designed to ensure that it does not cause further scour problems. Various types of scour protections are shown in Fig. 9 [6] for example: riprap protection, mattress protection, deflector and others. For riprap protection, it is the process of using stone or heavy material around the pier foundation to protect the bed material underneath the pier. However, this method does not perform well during floods or rain issue [11]. The mattress protection is widely used among the local and mostly use for a big circular pier in a fine bed material (sand). In general, special attention has to be given to providing a tight connection between the mattress and the pier, because even through a small gap, the downflow can induce severe erosion that extends under the mattress [10]. For the deflector, it aims to intently reduce the downflow from using material to block or change the streamline of the fluid flow when it hits the pier. No design rules are available for the determination of the width and the height of the deflector, which is fixed to the pier. Also, various type of shape and configuration of the deflector was designed. For example: collar deflector, scarified pile or submerged vane.

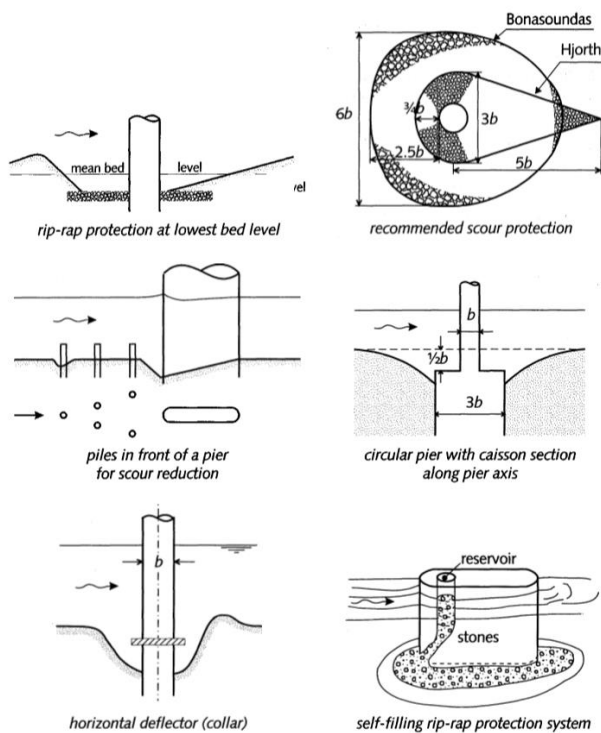


Fig. 9 Example of scour protections [6]

## 3. Material and Method

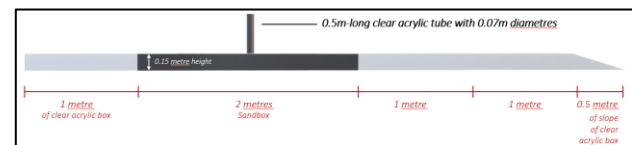
### 3.1 Setup test facilities

A series of laboratory experiments were performed in a rectangular large-sized open-channel flume in hydraulic laboratory of civil engineering department at King Mongkut's University of Technology Thonburi. The dimensions of the flume are 12-meter length, 0.6-meter width and 0.9-meter height with side walls comprised of steel frames and toughened glasses as shown in Fig. 10.

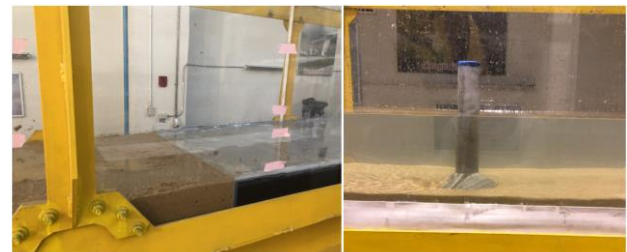


Fig 10 The experimental setup at KMUTT

There is a scour section in the large-sized current flume, which is 2 m length, 0.6 m width, 0.15 m depth as shown in Fig. 11 (a). There are clear acrylic boxes installed to build up the sediment section. The existing bed material level is elevated by 15 cm, which is prepared a 2 m length erodible bed in the middle of the flume section and is filled with designed sediment. Some part of experimental sand section is shown in Fig. 11 (b).



(a)



(b)

Fig. 11 The experimental sand section (a) sketch (b) real experiment

The median particle size ( $d_{50}$ ) of the natural sand used in the experiment is 0.40 mm. and the density of the river sediment is 2.65 g/cm<sup>3</sup>. Lee and Sturm had tested similar cases and recommend that the ration between pier diameter (D) and the

median particle size ( $d_{50}$ ) should be bigger than 25 ( $D/d_{50} > 25$ ) [12]. Since  $D/d_{50}$  of this experiment was more than 25 ( $D/d_{50} = 150$ ), the effect of sediment size on the scour hole can be negligible.

### 3.2 Design hydraulic characteristics

In order to conduct the experimental setup properly, some of the hydraulic characteristics need to be calculated and designed. The discharge and water depth were depicted by the following study of Chiew that the criterion proportion of water depth and pier model diameter in laboratory experiment should be more than 3 ( $d_f/D > 3$ ) [13]. Therefore, the ratio between water depth and pier model diameter ( $d_f/D$ ) equals to 3.44 which is bigger than the requirement ( $d_f/D > 3$ ). The experiments were conducted to use a constant flow discharge of  $0.045 \text{ m}^3/\text{s}$ .

Since there are two types of scour classification especially for the general and local scour based on their movement. To measure the type of scour, it was crucial to calculate flow intensity of  $v$  divided by  $V_c$  ( $v/V_c$ ) where  $v$  is the average velocity of the flow and  $V_c$  is the critical flow velocity for sediment movement. Clear water scour conditions occur when the ratio of flow intensity is less than 1 ( $v/V_c < 1$ ). Live-bed scour exists when the ratio of flow intensity is more than 1 ( $v/V_c > 1$ ). In this test, after calculate the ratio of flow intensity, the value obtained is 1.26 so, all the experiments perform under live-bed scour condition confirmed by the calculation mentioned above. To calculate the critical velocity ( $V_c$ ), it can be computed based on Eq. (1) [14].

$$\frac{V_c}{U_{*c}} = 5.75 \log\left(\frac{d_f}{d_{50}}\right) \quad (1)$$

Where  $V_c$  is the critical velocity (m/s),  $U_{*c}$  is the critical shear velocity of the bed materials based on  $d_{50}$  (m/s),  $d_{50}$  is median particle size of the sand (m) and  $d_f$  is flow depth above bed sediment (m).

Since  $U_{*c}$  is the critical shear velocity of bed materials based on  $d_{50}$ , to obtain the value, Shields diagram for the respective sizes of shear velocities needed to be determined as shown in Eq. (2).

$$U_{*c} = 0.0115 + 0.0125d_{50}^{1.4} \quad (2)$$

When  $0.1 \text{ mm} < d_{50} < 1 \text{ mm}$ . The critical shear velocity and the critical velocity and other important one was calculated

under the condition of the experiment. These characteristics as well as other essential ones have been summarized in Table 2.

**Table 2** Experimental conditions and hydraulic characters used in the present study.

Parameters	Unit	Value
Pier diameter (D)	m	0.6
Discharge (Q)	$\text{m}^3/\text{s}$	0.045
Flow depth ( $D_f$ )	m	0.204
Flow velocity (v)	m/s	0.376
$D/d_{50}$	-	150
Reynold number (Re)	-	89902
Froude number (Fr)	-	0.27
Critical velocity ( $V_c$ )	m/s	0.298
Critical shear velocity ( $U_{*c}$ )	m/s	0.015
Flow intensity ( $v/V_c$ )	-	1.26

### 3.3 Design based ramp protection models

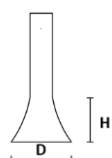
model prevents local scour by preventing the formation of scouring vortices over and around bridge piers. In addition, the shape of the based ramp model will help preventing the formation of scouring vortices and their highly fluctuating velocities and pressures.

Experiments were conducted to four different based ramp configurations shown in Fig. 12 and one unprotection case. A series of experiments was tested to investigate the effect of based ramp parameter. Table 3 lists all the dimensions and parameters carried out in this experiment. According to the pre-experimental checkup including the size of prototype models and experimental facilities, a live-bed scour testing scheme was adopted in this test and the working conditions of  $0.204 \text{ m}$  flow depth and  $0.045 \text{ m}^3/\text{s}$  discharge were selected.



**Fig. 12** The 4 configuration models of pier with based ramp

**Table 2** Experimental conditions and hydraulic characters used in the present study.

Characteristics	Cases				
	R5	R4	R3	R2	R1
Pier model	R5	R4	R3	R2	R1
Ramp diameter D (m)	-	0.16	0.16	0.16	0.16
Ramp height H (m)	-	0.16	0.12	0.08	0.04
Ratio H/D	-	1	0.75	0.50	0.25
Curve equation	-	$Y=0.16x^2$	$Y=0.32x^2$	$Y=0.48x^2$	$Y=0.64x^2$
Sketch drawing					

### 3.4 Setup numerical simulation model for drag coefficient determining

In order to figure out the reason behind the result of the laboratory experiment, a numerical simulation using ANSYS/FLUENT software (FLUENT,2018) has been developed for circular cylinder, representing bridge piers, to investigate the drag coefficient. This numerical simulation is focused on the water as running fluid around the pier, as a non-structure solid object, in order to calculate the drag coefficient, caused by water flow, of each based ramp model on the submerged pier model. Drag coefficients as shown in Eq. (3) are defined by using a characteristic area, in this case the frontal area of the based ramp pier models has been used.

$$F_d = \frac{1}{2} \rho v^2 C_d A \quad (3)$$

Where  $F_d$  is drag force (N),  $C_d$  is drag coefficient,  $\rho$  is density of fluid ( $\text{kg/m}^3$ ),  $v$  is velocity (m/s) and  $A$  is frontal area of the pier ( $\text{m}^2$ ). Once the program and the parameter were set up in the ANSYS/FLUENT software, the drag coefficient and the drag force will be calculated by the program as shown in Fig. 13.

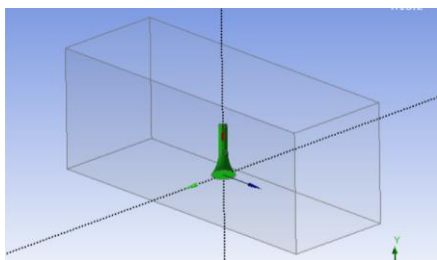


**Fig. 13** Water flow domain and based ramp pier model (R4)

## 4. Results and Discussions

After all the experiment has been done, the scour characteristic as maximum scour depth was observed and collected. The impact of various factors on scour characteristics and relate exchanges is discussed as follows:

### 4.1 The depth evolution of scour hole around bridge pier models

In order to measure the scour depth, the depth gauge is used to measure how deep is the scour hole in each of measuring points and then compare to find the maximum scour depth in each section. According to the scour hole development develops by the function of time, the measuring points were recorded every 10 minutes in the first 30 minutes, and then the measuring points were recorded every 30 minutes until it reaches 2 hours.

The maximum dimensionless scour depth  $S_d/S_{d,max}$  around the pier models as a function of scour testing time is given in Fig. 14. Scour occurred rapidly in the first 10 minutes especially for the unprotection case (R5) which reaches almost 40% of the maximum scour depth at 120 minutes within 10 minutes. R1 and R2 start at the same lowest amount of scour hole and performed in the similar trend in the middle of the period and finally resulted in 31% and 38% in the end of the period respectively (R1 presents the lowest maximum scour depth at all time). Although scour still occurred in the latter period, the rate of growth of the maximum scour depth seemed to slow down when the testing time increased. The worst protection case is R4 and the size of the depth is only at 13% different compared to the unprotection case (R5).

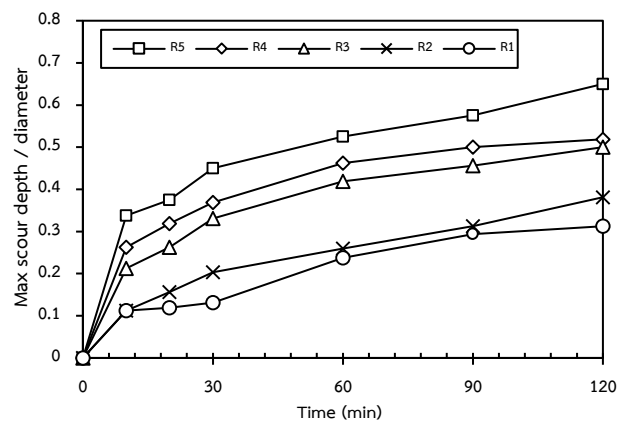


**Fig. 14** The maximum scour depth of each bridge pier model in each period.

#### 4.2 The scour depth protection efficiency of each bridge pier models

The effect of based ramp protection on the scour depth protective effect was experimentally investigated. The four different ratio of based ramp height and based (R1 - R4) were considered and compared to the unprotection case (R5). The protection efficiency of scour depth of each pier model defined as  $(S_{d,max} - S_{d,Ri}) / (S_{d,max}) * 100$ , Where the  $S_{d,max}$  is the maximum dimensionless depth of scour hole of R5 pier model at 120 minutes and  $S_{d,Ri}$  is the dimensionless depth of scour hole of each based ramp pier model (R1-R4) at 120 minutes is plotted in Fig. 15. It is obvious that the ratio of different based ramp configuration affects the scour depth protection efficiency significantly. The protection effect is increased with the decrease of based ramp height configuration. R1 or 4-cm based ramp is by far the most protective among the others at 51.9 percent, and this was followed by the R2 or 8-cm based ramp, at 41.3%. For R3 and R4 were half less protective approximately at 23.1% and 20.2% respectively.

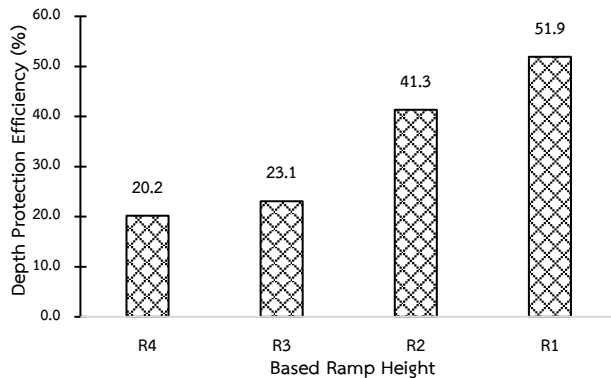


Fig. 15 The scour depth protection efficiency of each based ramp

#### 4.3 Drag coefficient simulation by numerical model

According to the text result of Vijayasree, et al. [15]. They have also found that the reduction of frontal areas of pier shape decreases the scour depth consistency and also the scour volume decreases with a decrease in the plan area. In order to find the support reason of the experiment results, All the based ramp configurations were modelled and developed in FLUENT. The models of 16 cm pier pillar with 4 different based ramp configurations were modelled in the fluid flow domain confined in a cuboid with the size of 2 x 0.8 x 0.6 (m) in x, y and z directions as shown in Fig. 16.

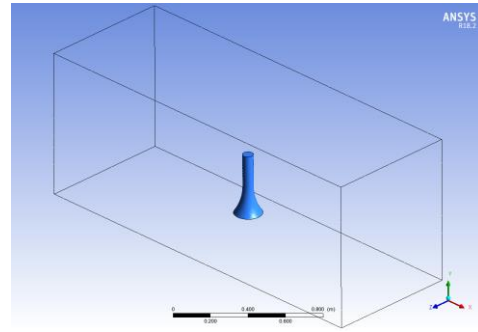


Fig. 16 The based ramp model on the designed fluid flow domain

As the characteristic of the structure was neglected in the process, the non-structured models were used to model the based ramp pier. In addition, the pier's boundaries were assumed to be non-slip walls, as was the channel walls boundary condition. For the Eulerian model, FLUENT provides mixture turbulence model in multiphase flows within the context of the k-ε models, also k-ε turbulence model is employed to simulate. The k-ε model was implemented in the Navier-Stokes flow solver, which was developed for turbulence models and is usually used for problems of solid/fluid interactions [16].

After the model validation was set, the drag coefficient and other related information including frontal area and force acting on pier of each based ramp configuration R1 - R5 were calculated as shown in Table 3. Therefore, the relation between drag coefficient of each based ramp model were plotted showing that R1 has the smallest amount of drag coefficient equal to 0.39 (dimensionless) and following by R2, R3 as 0.40 and 0.41 respectively. The R4 or 16-cm height-based ramp has the biggest coefficient of drag among other based ramp protection cases. Lastly, the R5 or unprotection bridge pier model has the biggest number of drag coefficient equal to 0.65 as shown in Fig. 17.

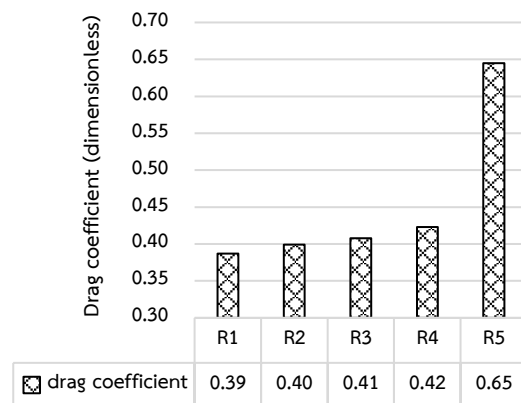


Fig. 17 The drag coefficient of based ramp configurations



**Table 3** The drag coefficient results and other related information.

Cases	Drag coefficient	Frontal area (m <sup>2</sup> )	Force (N)
R5	0.65	0.0512	0.5166
R4	0.42	0.0308	0.1958
R3	0.41	0.0289	0.1752
R2	0.40	0.0279	0.1652
R1	0.39	0.0270	0.1502

## 5. Conclusions

This research proudly presents a scour protection device around bridge pier using based ramp models by comparing the characteristic of the shape and its configuration in order to seek for the most effective and proper configuration of the based ramp. The scour mechanism and the time-varied development of scour depth was investigated by carrying out laboratory tests. The scour depth protection efficiency was studied and discussed. Also, the drag coefficient and frontal area of the based ramp models were simulated by the numerical simulation program in order to support the characteristic of the experiment results. The main finding and analytical results, some conclusions can be drawn as follows:

The shape and the configuration of based ramp is an important parameter in the scour processing which result in different size and depth of scour hole. Based on the experimental results: the R1 or 0.25 H/D ratio is the most optimal case that can effectively reduce more than half of scour depth when compare to a pier without protection.

The based ramp protection has clear protective effect that the reduction of H/D ratio contribute to the increasing of the scour depth protection efficiency. In addition, the based ramp protection indicates scour depth protection as much as approximate 52%.

The simulation model reports that the decreasing of frontal area of pier contribute to the decreasing of drag coefficient resulting in better protective effects. In addition, the based ramp models create the coefficient of drag around 0.4

## Acknowledgement

The authors sincerely thank the family and friends for their valuable supports and also thank the hydraulic laboratory of department of civil engineering, King Mongkut's University of Technology Thonburi for the financial support and helps. Our research could not be accomplished without everyone supports.

## References

- [1] Richardson, E.V., Harrison, L.J., Richardson, J.R., and Davies, S.R. (1993). "Evaluating Scour at Bridges", Federal Highway Administration, US Department of Transportation: Publ. FHWA-IP-90-017, Washington, DC, USA, pp. 35-39.
- [2] Melville, B.W., Coleman, S.E. (2000). Bridge Scour, Water Resources Publication, Highlands Ranch, CO, USA, 2000.
- [3] Sheppard, D. M. and Renna, R. (2010). Bridge scour manual, 605 Suwannee Street. Tallahassee, FL 32399-0450.
- [4] Leeuwen, Z.V. and Lamb R. (2014). Flood and scour related failure incidents at railway assets between 1846 and 2013, 1st, JBA Trust Limited, North Yorkshire BD23 3AE United Kingdom, pp. 4-20.
- [5] Hoffmans, G.J.C.M. and Verheij, H.J. (1997). Scour Manual, 2nd ed., Taylor & Francis, Rotterdam, Netherlands, p. 117.
- [6] Breusers, H.N.C. and Raudkivi, A.J. (1991) Scouring. Balkema, Rotterdam, NL.
- [7] Yeleğen, M. Ö. and Uyumaz, A. (2016). Flow Velocity Effect on Clear Water Bridge Pier Scour", The World Congress on Civil, Structural and Environmental Engineering, Prague, Czech Republic, No. ICESDP 103
- [8] Dargahi, B. (1987) Flow field and local scouring around a cylinder. Bulletin TITRA- VBI-137, Department of Hydraulics Engineering, Royal Institute of Technology, Stockholm, Sweden.
- [9] Carstens, T. (1976) Seabed scour by currents near platforms, 3rd Conference on port and ocean engineering under arctic conditions, University of Alaska: 991-1006.
- [10] Beg, M. and Beg, S. (2013). Scour Reduction around Bridge Piers: A Review, International Journal of Engineering Inventions, PP: 07-15
- [11] Lee, S.O., and Sturm, T.W., 2009, "Effect of sediment size scaling on physical modelling of bridge pier scour. Journal of hydraulic engineering, pp. 86-89
- [12] Chiew Y. M., 1995, "Mechanics of riprap failure at bridge piers", Journal of hydraulic engineering, pp. 23-36.
- [13] Mellville, B. W. (1997). Pier and abutment scour. Integrated approach. Journal of hydraulic engineering, 132(2), 125-136.
- [14] Vijayasree, B. A., Eldho, T. I., Mazumder, B. S. and Ahmad, N. (2017). Influence of bridge pier shape on flow field and scour geometry, International Journal of River Basin Management, Taylor & Francis Group.

- [15] Kok, J. C. and Spekreijse, S. P. (2000). Efficient and accurate implementation of the k-omega turbulence model in the NLR multi-block Navier-Stokes system, Amsterdam: Nationaal Lucht-en Ruimtevaartlaboratorium, pp. 150-165.